

FAST MUSCLE FUNCTION IN THE EUROPEAN EEL (*ANGUILLA ANGUILLA* L.) DURING AQUATIC AND TERRESTRIAL LOCOMOTION

D. J. ELLERBY^{1,*}, I. L. Y. SPIERTS² AND J. D. ALTRINGHAM¹

¹*School of Biology, University of Leeds, Leeds LS2 9JT, UK* and ²*Experimental Zoology Group, Department of Animal Sciences, Wageningen Institute of Animal Sciences, Wageningen University, The Netherlands*

*Author for correspondence at present address: Department of Biology, 414 Mugar, Northeastern University, Boston, MA 02115, USA
(e-mail: dellerby@lynx.neu.edu)

Accepted 9 April 2001

Summary

Eels are capable of locomotion both in water and on land using undulations of the body axis. Axial undulations are powered by the lateral musculature. Differences in kinematics and the underlying patterns of fast muscle activation are apparent between locomotion in these two environments. The change in isometric fast muscle properties with axial location was less marked than in most other species. Time from stimulus to peak force (T_a) did not change significantly with axial position and was 82 ± 6 ms at $0.45BL$ and 93 ± 3 ms at $0.75BL$, where BL is total body length. Time from stimulus to 90% relaxation (T_{90}) changed significantly with axial location, increasing from 203 ± 11 ms at $0.45BL$ to 239 ± 9 ms at $0.75BL$. Fast muscle power outputs were measured using the work loop

technique. Maximum power outputs at $\pm 5\%$ strain using optimal stimuli were 17.3 ± 1.3 W kg⁻¹ in muscle from $0.45BL$ and 16.3 ± 1.5 W kg⁻¹ in muscle from $0.75BL$. Power output peaked at a cycle frequency of 2 Hz. The stimulus patterns associated with swimming generated greater force and power than those associated with terrestrial crawling. This decrease in muscle performance in eels may occur because on land the eel is constrained to a particular kinematic pattern in order to produce thrust against an underlying substratum.

Key words: European eel, *Anguilla anguilla*, locomotion, muscle, power output, kinematics, swimming, crawling.

Introduction

Eels are unusual amongst teleost fish in being able to make brief terrestrial excursions (Gray, 1968; Lindsey, 1978). Both swimming and crawling involve undulations of the body axis that are powered by the lateral musculature (Gillis, 2000). Muscular contraction, the interactions between the fish and the water or substratum, and the mechanical properties of the passive components of the body combine to produce a wave of curvature that passes along the body axis. The body/tail wave generates net thrust. Teleost fish exhibit variation in the patterns of muscle strain and activation during locomotion both among species and with axial position in a given species (Grillner and Kashin, 1976; Williams et al., 1989; van Leeuwen et al., 1990; Wardle and Videler, 1993; Johnson et al., 1994; Jayne and Lauder, 1995; Hammond et al., 1998; Ellerby et al., 2000). Studies of isolated muscle fibres from a number of fish species have shown that the phase relationship between strain and activation is crucial in determining the mechanical output of the muscle (Altringham et al., 1993; Rome et al., 1993; Wardle et al., 1995; Curtin and Woledge, 1996; Hammond et al., 1998; Altringham and Ellerby, 1999).

Axially, the lateral musculature is divided into a series of myotomes. In fish, different muscle fibre types with distinct properties are usually arranged in discrete populations within

each myotome. Sustained locomotion at low tailbeat frequencies is powered by slow-twitch aerobic muscle (e.g. Bone, 1966; Rayner and Keenan, 1967; Rome et al., 1992; Coughlin and Rome, 1999). Fast-twitch fibres are recruited during fast starts and bursts of swimming at a high tailbeat frequency (e.g. Rayner and Keenan, 1967; Johnston et al., 1977). Fast fibres are also recruited during terrestrial locomotion in eels (Gillis, 2000).

In some teleosts with a distinct caudal fin, there may be subtle changes in muscle function along the body axis during swimming (e.g. van Leeuwen et al., 1990; Altringham et al., 1993; Altringham and Ellerby, 1999). Caudal fast muscle may produce some negative work and have a role in power transmission as well as power production. Also, in most teleosts studied, muscle properties are known to change along the body: muscle kinetics slow down from head to tail, but the link between these observations remains unexplained (Altringham and Ellerby, 1999). It has been hypothesised that muscle properties and muscle function may be more homogeneous along the body of an eel than in fish with a distinct caudal fin. This is because thrust is thought to be produced more uniformly along the body axis rather than primarily in the caudal region (Wardle et al., 1995; D'Aouit and

Aerts, 1999). The isometric properties of the fast muscle of the European eel *Anguilla anguilla* L. were measured at two points along the body axis to test for uniformity of muscle kinetics. To determine whether the caudal musculature produced any negative work that could be associated with a power-transmitting mechanism, the work loop technique (Josephson, 1985) was used to measure axial patterns of power production under approximated *in vivo* conditions.

Locomotion in a buoyant three-dimensional fluid medium probably requires different patterns of muscle function from locomotion on a two-dimensional solid surface. It has been shown that the body kinematics (Gillis, 1998a) and patterns of fast muscle activity (Gillis, 2000) in an eel are different between locomotion on land and in the water. We have also determined how the activation patterns associated with these two different modes of locomotion affect force production and power output in the fast muscle. Patterns of force and power production are discussed in relation to the differing demands of aquatic and terrestrial locomotion.

Materials and methods

European eels (*Anguilla anguilla* L.) were obtained from commercial fishermen. The fish were caught using nets in the freshwater fenland drains of south Lincolnshire, UK. Mean body mass was 284 ± 24 g, and mean body length was 552 ± 15 mm ($N=12$, means \pm S.E.M.). Eels undergo various physiological and anatomical changes prior to migration, changing from the non-migratory yellow phase to the migratory silver phase (e.g. Eggington, 1987). The life-history phase was determined on the basis of an eye size index I :

$$I = 100 \left(\frac{\pi(A+B)^2/4}{BL} \right)$$

(Pankhurst, 1982), where A and B are horizontal and vertical eye diameters, respectively, and BL is body length (measurements in mm). Mean eye size index was 13.6 ± 0.7 (mean \pm S.E.M., $N=7$). This falls within the range reported previously (Ellerby et al., 2001) for *A. anguilla* yellow-phase eels. The fish were held in 2 m diameter fibreglass tanks that contained aerated, filtered water at a temperature of 14°C . A 16 h:8 h light:dark photoperiod was maintained in the aquarium. The eels were fed a maintenance diet of freeze-dried bloodworms three times a week.

Eels were killed by decapitation, destruction of the brain and pithing of the spinal cord. Blocks of skeletal muscle tissue were removed from the lateral line region. These were placed in oxygenated Ringer's solution (composition in mmol l^{-1} : NaCl, 109; KCl, 2.7; NaHCO_3 , 2.5; CaCl_2 , 1.8; MgCl_2 , 0.47; sodium pyruvate, 5.3; Hepes, 10; pH 7.4 ± 0.05 at 14°C) cooled to 8°C . The tissue blocks were pinned out, and any slow muscle fibres, fat and skin were rapidly removed. The Ringer's solution was replaced frequently during dissection. The resulting muscle preparations consisted of bundles of fast muscle fibres from the superficial anterior-pointing cones of the myotomes. These

Table 1. Approximated *in vivo* stimulus parameters

	Swimming		Crawling	
	Onset (degrees)	Duty cycle (degrees)	Onset (degrees)	Duty cycle (degrees)
0.45BL	77	103	121	146
0.75BL	70	68	101	133

Stimuli were derived from the electromyographic data of Gillis (2000) for American eel (*Anguilla rostrata*).

Stimulus onset was measured relative to a 360° sinusoidal strain cycle. At $0^\circ/360^\circ$, the preparation was at l_0 and lengthening, where l_0 is the preparation length that yielded maximum isometric stress.

Duty cycle is the duration of the stimulus relative to the strain cycle.

BL, total body length.

were approximately 0.3 mm^2 in cross-sectional area and 3–4 mm in length and ran between two collagenous myosepta. They were connected directly to hooks on the servo arm and force transducer (AE801, SensoNor, Horten, Norway) via the connective tissue of the myosepta. Each muscle preparation was then allowed to recover for 1 h. The preparations were bathed in recirculating, oxygenated Ringer's solution at 14°C . The work loop apparatus and techniques were as described previously (e.g. Altringham and Johnston, 1990; Hammond et al., 1998).

Stimulus amplitude (2 ms pulse) was adjusted to 120% of that giving a maximal response. The fibre length was then increased in increments of 0.2 mm using a micromanipulator until the preparation yielded a maximal twitch response. This was taken as resting length (l_0) and corresponded closely to the resting fibre length in the fish when lying flat. A 2 ms stimulus was used to compare the twitch kinetics of fibres from different axial locations. The activation time T_a , the time from stimulus onset to peak force, and T_{90} , the time from stimulus onset to 90% relaxation, were measured. Tetanic stimulus frequency was adjusted to that yielding a maximum tetanic response (approximately 80 Hz).

Muscle preparations were subjected to sinusoidal length changes. *In vivo* strain patterns in swimming fish are approximately sinusoidal (e.g. Hammond et al., 1998; Knower et al., 1999; Ellerby et al., 2000). Muscle preparations were subjected to strain cycles of $\pm 5\%$ l_0 . *In vivo* eel fast muscle strains are unknown. Calculated superficial strains ranged from approximately ± 5 to $\pm 12\%$ l_0 in *A. anguilla* during forward swimming and were as high as $\pm 25\%$ l_0 during backward swimming (D'Août and Aerts, 1999). Because of fibre geometry and greater proximity to the backbone, fast muscle strains are thought to be lower than superficial slow muscle strains (Alexander, 1969).

Stimulus parameters are expressed in degrees relative to the 360° sinusoidal strain cycle where the muscle is at resting length l_0 and lengthening at 0° . Approximated *in vivo* stimulation parameters were derived from Gillis (Gillis, 2000) (Table 1). These data related to *Anguilla rostrata* not *A.*

anguilla. These two Atlantic eel species cannot be unambiguously separated on the basis of morphology or enzyme electrophoresis (Williams and Koehn, 1984). There are small differences in mitochondrial DNA sequences (e.g. Avise et al., 1990) that separate the two species, but the difference between *A. anguilla* and *A. rostrata* is only slightly greater than the variation displayed within *A. anguilla* (Bastrop et al., 2000). On the basis of this high degree of similarity, it seemed reasonable to use these parameters to approximate the *in vivo* stimulus patterns of *A. anguilla*. The stimulus parameters required for maximum power production were obtained by systematically altering stimulus onset phase and duration relative to the strain cycle.

The muscle preparations were subjected to experimental runs of five cycles. Work and power were calculated using the work loop technique (e.g. Josephson, 1985; Altringham and Johnston, 1990). Power output stabilised after the first cycle. Work and power output measurements were derived from the third cycle. Preparations were allowed to rest for 10 min between experimental runs to minimise fatigue. On completion of an experiment, the preparations were removed from the chamber. Each preparation was viewed using a binocular microscope, and the connective tissue of the myosepta and the dead cells were cut away. The remaining tissue was blotted to remove excess Ringer's solution prior to weighing. Cross-sectional area was calculated as volume/length of the preparation, where volume was determined assuming a value for muscle density of 1060 kg m^{-3} .

To detect any change in muscle performance during the experiment, preparations were subjected to a control trial, with fixed parameters (cycle frequency 2 Hz, strain $\pm 5\%$, stimulus onset 60° and stimulus duration 100°) after every fourth run. Power outputs were scaled relative to these control trials. After a small decrease in power output during the initial stages of the trial, power output stabilised and remained virtually constant for the remainder of the experiment (up to 6 h in total).

Statistical analyses

Statistical analyses were carried out using SigmaStat (SPSS, Chicago, IL, USA) software. Basic muscle mechanical properties were tested for significant differences between body positions using a Student's *t*-test. Power and work outputs were tested for significant differences between stimulus regimes using analysis of variance (ANOVA). Significant differences were measured using the Student–Newman–Keuls test. Values are given as means \pm S.E.M.

Results

Isometric properties of eel fast muscle

The time from stimulus to peak twitch force (T_a) did not differ significantly with axial position. Time from stimulus to 90% relaxation (T_{90}) was significantly greater in the posterior fast muscle than in the anterior fast muscle. Maximum tetanic isometric stress was not significantly different in fast muscle

Table 2. The isometric properties of eel fast muscle

Position	0.45BL	0.75BL	<i>P</i>
Time from stimulus to peak force, T_a (ms)	82.0 \pm 6.3	92.5 \pm 3.2	0.172
Time from stimulus to 90% relaxation, T_{90} (ms)	202.5 \pm 10.5	239.0 \pm 8.6	0.022
Maximum isometric stress (kN m^{-2})	140.2 \pm 13.2	143.0 \pm 16.0	0.867
Twitch:tetanus ratio	0.40 \pm 0.05	0.38 \pm 0.08	0.766

Values are shown as mean \pm S.E.M. ($N=6$).

Probability values are those returned a by Student's *t*-test used to compare the values from different axial locations.

BL, total body length.

from the two axial positions. Similarly, the ratio of isometric twitch force to tetanic force did not differ significantly with body position. The mechanical properties of eel fast muscle are summarised in Table 2.

Fast muscle power output

Stimulus duration and onset phase were systematically changed until maximum power output was achieved for a given cycle frequency. Optimal stimulus onset did not change significantly with body position (two-way ANOVA, $P=0.607$) but did change significantly with cycle frequency (two-way ANOVA, $P<0.001$). Optimal stimulus onset was earlier relative to the strain cycle at higher cycle frequencies. Similarly, optimal stimulus duration did not change significantly with body position (two-way ANOVA, $P=0.497$) but did change significantly with cycle frequency (two-way ANOVA, $P<0.001$). Optimal stimulus duration decreased with increasing cycle frequency. There was little difference in the relationship between maximal power output of fast muscle and cycle frequency between muscle from 0.45 and 0.75BL (Fig. 1). Power output peaked at a cycle frequency of 2 Hz. Maximum power output was $17.3\pm 1.3 \text{ W kg}^{-1}$ in fast muscle from 0.75BL and $16.3\pm 1.5 \text{ W kg}^{-1}$ in fast muscle from 0.45BL. There was no significant difference in power output with body position (two-way ANOVA, $P=0.924$). Positive power output could not be achieved at cycle frequencies above 4 Hz.

Power outputs obtained with approximated *in vivo* stimuli are shown in Fig. 2. Under simulated swimming conditions, maximum power output was $10.0\pm 0.5 \text{ W kg}^{-1}$ in the anterior muscle and $10.5\pm 0.5 \text{ W kg}^{-1}$ in the posterior muscle. Maximum power output occurred at a cycle frequency of 1–2 Hz in the anterior muscle and of 1–3 Hz in the posterior muscle. Positive power output could not be achieved at cycle frequencies above 4 Hz. Under simulated crawling conditions, maximum power outputs were lower than those achieved during simulated swimming. Maximum power output was $5.6\pm 0.6 \text{ W kg}^{-1}$ and $8.9\pm 0.3 \text{ W kg}^{-1}$ in fast muscle from 0.45BL and 0.75BL respectively. When using simulated crawling parameters, peak power output occurred at cycle frequencies

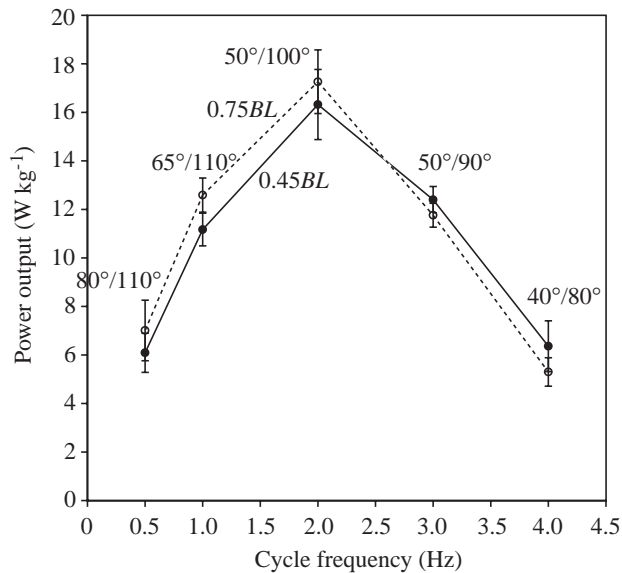


Fig. 1. Mean power output of eel fast muscle *versus* cycle frequency under optimal stimulus conditions and a strain of $\pm 5\%$. Values are means \pm S.E.M. ($N=6$). Optimal stimulus at a given frequency is shown as onset/duty cycle in degrees. Stimulus onset was measured relative to a 360° sinusoidal strain cycle. At $0^\circ/360^\circ$, the preparation was at l_0 and lengthening, where l_0 is the preparation length that yielded maximum isometric stress. Data from $0.45BL$ are shown as filled circles with a solid line, data from $0.75BL$ are shown as open circles with a dashed line. BL , total body length.

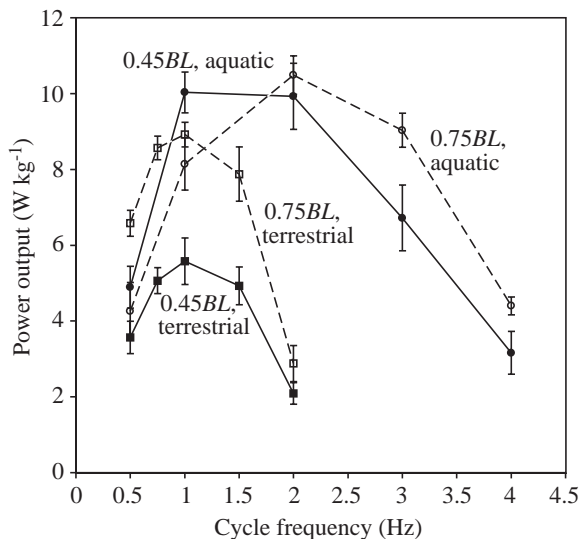


Fig. 2. Mean power output of eel fast muscle *versus* cycle frequency under approximated *in vivo* stimulus conditions and a strain of $\pm 5\%$. Values are means \pm S.E.M. ($N=6$). Filled symbols represent data from muscle at $0.45BL$, and open symbols represent data from muscle at $0.75BL$. Squares represent data obtained using approximated terrestrial stimulus parameters, and circles represent data obtained using approximated aquatic stimulus parameters. Stimulus parameters were obtained from Gillis (Gillis, 2000). BL , total body length.

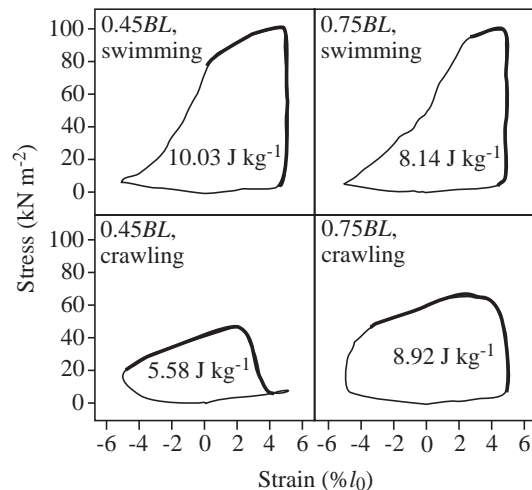


Fig. 3. Representative work loops obtained using *in vivo* stimulus parameters measured by Gillis (Gillis, 2000). The thickened regions of the loops show when the muscle preparation was activated. All loops were obtained at a cycle frequency of 1 Hz. Mean work outputs ($N=6$) are shown within each loop. BL , total body length.

of 0.5–1.5 Hz in fast muscle from both axial positions. Positive power output could not be achieved above cycle frequencies of 2 Hz. Representative work loops are shown in Fig. 3.

Time course of force and power production

The timing of peak stress was significantly later relative to the strain cycle during simulated crawling than during simulated swimming in muscle from both body positions (two-way ANOVA, $P<0.001$). Peak stress occurred significantly later in the anterior muscle than in the posterior muscle during simulated crawling (Student–Newman–Keuls test, $q=3.6$, $P<0.05$), but not during simulated swimming (Student–Newman–Keuls test, $q=4.9$, $P>0.05$). The magnitude of peak stress did not differ significantly with body position either during simulated crawling or during simulated swimming (Student–Newman–Keuls test, $q=4.7$ (swimming), $q=2.9$ (crawling), $P>0.05$). Peak stresses were significantly higher during swimming than during crawling (two-way ANOVA $P<0.05$). The time course of stress and power production during the strain cycle differed between simulated swimming and crawling (Fig. 4, Fig. 5). High stresses persisted much later into the strain cycle in crawling compared with swimming (Fig. 4). There was a similar pattern in the time course of power output (Fig. 5). The majority of power and work production was positive at both axial positions and under both stimulus regimes. The timings and magnitudes of peak stresses during the strain cycle using approximated *in vivo* stimuli are summarised in Table 3.

Discussion

Isometric properties

The isometric twitch relaxation times changed with axial

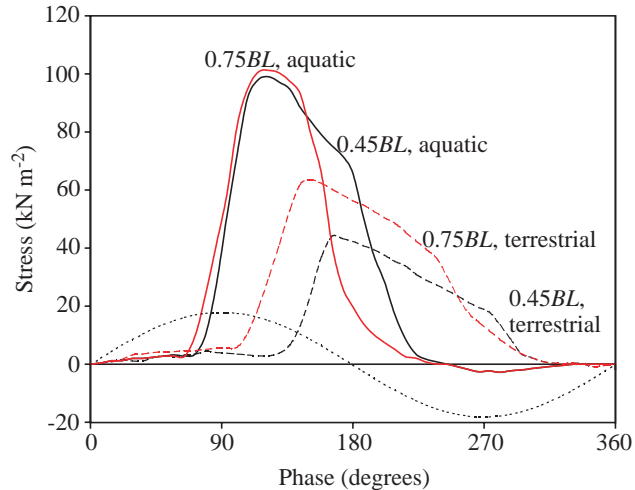


Fig. 4. Representative traces showing fast muscle stress during a single sinusoidal strain cycle (strain $\pm 5\%$). Solid lines represent stress during simulated swimming, and dashed lines represent stress during simulated crawling. Black traces show stress in preparations from 0.45BL and red traces show stress in preparations from 0.75BL. The dotted line represents muscle length. BL, total body length.

position (Table 2). A similar increase in contraction time moving in a rostro-caudal direction has been measured in the fast muscle of some other teleost species (bluefin tuna *Thunnus thynnus*, Wardle et al., 1989; saithe *Pollachius virens*, Altringham et al., 1993; cod *Gadus morhua*, Davies et al., 1995). It has been hypothesised that axial muscle properties are relatively uniform in the eel because thrust is thought to be produced uniformly along the body axis rather than primarily in the caudal region (Wardle et al., 1995; D'Août and Aerts, 1999). Although the lateral fast muscle of the eel was not homogeneous, the degree of change in muscle properties along the body axis was smaller than in these species. Altringham et al. (Altringham et al., 1993) found a twofold increase in twitch T_{90} between 0.35 and 0.65BL in saithe, and tetanic activation and relaxation times increased by up to 70% between 0.35 and 0.65BL in the cod (Davies et al., 1995). This compares with an increase in T_{90} of only 18% between 0.45 and 0.75BL in the eel and no significant increase in T_a . The exception to this general pattern is the sculpin (*Myoxocephalus scorpius*), in which tetanic activation and relaxation times do not change with axial location (Johnston et al., 1993). The sculpin

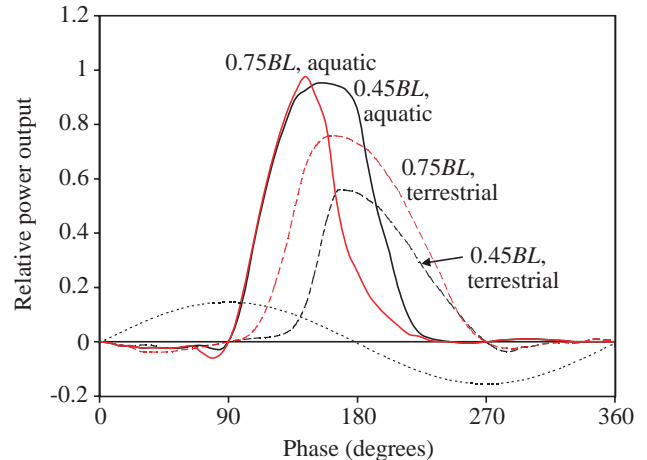


Fig. 5. Representative traces showing relative instantaneous fast muscle power output during a single sinusoidal strain cycle (strain $\pm 5\%$). Solid lines represent instantaneous power output during simulated swimming, and dashed lines represent instantaneous power output during simulated crawling. Black traces show stress in preparations from 0.45BL and red traces show stress in preparations from 0.75BL. The dotted line represents muscle length. Power outputs are scaled relative to peak instantaneous power at 0.75 BL under simulated swimming conditions.

possesses a distinct caudal fin. It seems that the presence or absence of a caudal fin and the resulting patterns of thrust production are not the only factors determining axial muscle properties.

Maximum isometric tetanic stresses were within the range measured in other teleost fast muscle. Eggington (Eggington, 1987) measured a maximum isometric stress of 102 kN m^{-2} in single fast fibres of the yellow-phase American eel, lower than that (140 kN m^{-2}) measured in the present study. Isometric tetanic stresses were comparable with those measured (Altringham et al., 1993) in the fast muscle of the saithe (*Pollachius virens*, $136\text{--}151 \text{ kN m}^{-2}$).

Fast muscle power output

The maximum fast muscle power outputs of $16\text{--}17 \text{ W kg}^{-1}$ measured in the present study were lower than those measured in the fast muscle of other teleosts. Maximum fast muscle power output was 63 W kg^{-1} in the saithe (*Pollachius virens*) (Altringham et al., 1993) and 35 W kg^{-1} in the sculpin

Table 3. The timing of peak fast muscle stresses relative to the strain cycle during simulated swimming and crawling

Stimulus regime	0.45BL		0.75BL	
	Swimming	Crawling	Swimming	Crawling
Timing of peak stress relative to the strain cycle at 1.0 Hz (degrees)	119 \pm 4	172 \pm 6	113 \pm 8	152 \pm 6
Peak stress during strain cycle at 1.0 Hz (kN m^{-2})	107 \pm 30	74 \pm 18	111 \pm 30	45 \pm 11

Timings are relative to a 360° sinusoidal strain cycle. At $0^\circ/360^\circ$ the preparation was at l_0 and lengthening, where l_0 was the preparation length that yielded maximum isometric stress.

Data are shown as mean \pm S.E.M. ($N=6$).

BL, total body length.

(Altringham and Johnston, 1990). The power requirements of swimming scale to approximately the third power of swimming speed (Webb, 1978). The low power output of eel fast muscle suggests that the maximum swimming speed must be low relative to that of these other teleosts. The only previous measurement of eel muscle power output was obtained using whole-body work loop experiments on the American eel (Long, 1998) in which the maximum power output measured was 23 W kg^{-1} . The entire lateral musculature in the caudal region was stimulated at a cycle frequency of 3 Hz. As the majority of the lateral musculature is made up of fast fibres, this was effectively a measure of fast muscle power output. The relative stimulus duration used by Long (180°; Long, 1998) was much greater than that measured *in vivo* (Gillis, 2000, Table 1). Maximum power output was achieved at a stimulus onset of 325° relative to the strain cycle. The optimal stimulus onset/duration at 3 Hz in isolated fibres in the present study was 50°/90°. In isolated muscle preparations, a stimulus onset of 325° early in the lengthening phase would result in a large negative work component during the strain cycle and a low net work output. Long (1998) suggested that this activation pattern stretched a series elastic component within the lateral musculature which returned energy later in the strain cycle. The disparity between the optimum stimulus onset for power output using isolated fibres and whole-body work loops highlights the fact that the interactions between the muscle fibres and their mechanical environment in the intact fish are complex and poorly understood.

Despite the longitudinal differences in isometric properties, there are no apparent differences with axial position in the optimal stimulation parameters required for maximum power output or the relationship between power output and cycle frequency. The cycle frequency yielding maximum power output (2 Hz) was much lower in eel fast muscle than in the fast muscle of other fish. For example, peak frequency was 8 Hz in the saithe (Altringham et al., 1993) and 5–7 Hz in the sculpin (Altringham and Johnston, 1990). Power output is the product of cycle frequency and the work output per cycle. The low operating frequency of eel fast muscle accounts for its low power output relative to other teleosts. Work output provides a means for comparing fast muscle performance with that of other teleosts because it removes the influence of cycle frequency. At peak power output (cycle frequency 2 Hz) under optimal stimulus conditions, the work output per cycle of eel fast muscle was 8.2 J kg^{-1} in the anterior muscle and 8.6 J kg^{-1} in the posterior muscle. The work output of saithe muscle at maximum power output was 7.9 J kg^{-1} (Altringham et al., 1993), and that of the sculpin was 7.0 J kg^{-1} (Altringham and Johnston, 1990). On this basis, the performance of eel fast muscle is comparable with that of other teleost fast muscle.

There was no substantial negative work or power component during the strain cycle (Fig. 5). A small amount of negative work was associated with activation whilst lengthening under swimming stimulus conditions. A large negative work component has been measured or calculated during the strain cycle in the caudal muscle of some teleosts. It has been

suggested that this may stiffen the caudal muscle during part of the strain cycle as a means of power transmission from more anterior muscle to the caudal fin (van Leeuwen et al., 1990; Altringham et al., 1993). The lack of substantial negative power and work production in eel caudal fast muscle suggests that there is no reliance on stiffened fast muscle for power transmission along the body axis. This is consistent with the view of relative uniformity of muscle function and limited requirements for axial power transmission in anguilliform swimmers where thrust is generated along much of the body axis rather than by a caudal fin (Wardle et al., 1995; Altringham and Ellerby, 1999).

Why is the operating frequency of eel fast muscle lower than that of other fish? The twitch activation times (T_a , 82–93 ms) were longer than those measured in the fast muscle of the saithe. T_a in the saithe ranged from 27 to 44 ms (Altringham et al., 1993). Relaxation times were also relatively longer in eel fast muscle. T_{90} in the eel (203–239 ms) was also longer than that of the saithe (62–136 ms, Altringham et al., 1993). Relatively slow contraction times in eel fast muscle may impose an upper limit on the cycle frequency at which it can operate. In repeated length change cycles, failure of the preparation to relax fully before the subsequent cycle results in negative work production because stresses remain high during muscle lengthening.

Locomotory performance in water and on land

On the basis of *in vitro* patterns of power production at 14 °C, European eels could not attain a tailbeat frequency greater than 4 Hz during swimming. Direct comparisons with previous kinematic studies are complicated by temperature differences. In yellowfin tuna (*Thunnus albacares*) and bonito (*Sarda chiliensis*), a temperature rise from 15 to 20 °C resulted in a doubling of the cycle frequency at which peak power production was achieved (Altringham and Block, 1997). The highest tailbeat frequencies recorded in eels at 20 °C were approximately 4 Hz in *A. anguilla* (D'Août and Aerts, 1999) and 3.3 Hz in *A. rostrata* (Gillis, 1998b), although measuring the maximum possible tailbeat frequency was not the aim of these studies. If the temperature difference is accounted for, then at 20 °C the optimal cycle frequency for power production may be closer to 4 Hz. Grillner and Kashin (Grillner and Kashin, 1976) measured tailbeat frequencies of 5 Hz in *A. anguilla*, beyond the frequency range achieved *in vitro*. The temperature at which this occurred was not stated and may well have been higher than in the present study.

The maximum cycle frequency at which positive power output could be achieved *in vitro* was much lower under simulated crawling conditions (2 Hz). At cycle frequencies above 2 Hz, because of the relatively late stimulus onsets and durations, the muscle could not relax fully before the subsequent strain cycle. These *in vitro* measurements are consistent with kinematic observations: the highest cycle frequency recorded by Gillis (Gillis, 1998a) for *A. rostrata* on land was 1.3 Hz.

The stimulus parameters that maximised power production

(Fig. 1) were different from those measured *in vivo* for *A. rostrata* by Gillis (Gillis, 2000) (Table 1). Generating maximum power output is not necessarily the only consideration *in vivo*. The conditions for maximum efficiency, for example, can differ from those that generate maximum power output (Curtin and Woledge, 1996). The different stimulus patterns associated with swimming and crawling (Table 1) produced very different patterns of force and power production during the strain cycle (Fig. 4, Fig. 5). This was reflected in the shapes of the resulting work loops (Fig. 3). Higher peak stresses were generated by the activation patterns associated with swimming (Table 3; Fig. 4). This was because during simulated swimming the onset of muscle activity occurred in the lengthening phase just prior to maximum length. This type of activation pattern has been shown to enhance muscle force and power production during the subsequent shortening phase (e.g. Altringham and Johnston, 1990). The stimulus parameters required for maximum power output included onset of activation during lengthening (Fig. 1). During simulated crawling, the onset of muscle activity occurred during shortening, and force production was consequently lower.

Below a cycle frequency of 1 Hz, the stimulus patterns associated with crawling resulted in a greater power output in the posterior muscle than those associated with swimming (Fig. 2). However, above 1 Hz, power output was greater under simulated swimming conditions. In the anterior muscle, power output was always lower during simulated crawling than during simulated swimming. Why would a shift in stimulus patterns that in general results in an overall decrease in power and force production occur on transition to land? It is possible that locomotion on an unyielding surface may require the generation of less force than thrust generation in a fluid. However, fast muscle electromyographic intensity is greater on land than in water (Gillis, 2000). This suggests an increased recruitment of locomotor units that may, in part, offset the general reduction in fast muscle work and power output on land. Movement from an environment in which the body is no longer supported by buoyancy may also require greater force production. The greater degrees of body curvature and lateral displacement associated with crawling probably increase fast muscle strain. This may increase work and power production on land.

An explanation may lie in the shift in kinematics on transition to land. During swimming, not all parts of the body follow the same path: the amplitude envelope of the body increases from anterior to posterior (Gillis, 1998a; D'Août and Aerts, 1999; Ellerby et al., 2001). During terrestrial locomotion, all points on the body axis follow a similar path and when crawling on sand the body of the eel creates a groove in the substratum (Gillis, 2000). The posterior parts of the body follow the groove created by the anterior parts, and the groove may be used to improve traction. This is also the case during terrestrial crawling in snakes (Mosauer, 1932; Gray, 1946). If the kinematics remained the same as during swimming, then the eel would be unable to take advantage of this mechanism.

The shift in activation patterns and the resultant changes in force production may be related to this kinematic shift, making the associated loss in performance unavoidable if traction is to be maintained. It would be interesting to determine how different types of surface affect terrestrial kinematics and whether more solid surfaces in which a groove could not be produced would result in a different pattern of muscle function.

D.J.E. was supported by a BBSRC special studentship. I.L.Y.S. was supported by a grant from the Niels Stensen Foundation.

References

- Alexander, R. McN. (1969). The orientation of muscle fibres in the myomeres of fish. *J. Mar. Biol. Ass. U.K.* **49**, 263–290.
- Altringham, J. D. and Block, B. A. (1997). Why do tuna maintain elevated slow muscle temperatures? Power output of muscle isolated from endothermic and ectothermic fish. *J. Exp. Biol.* **200**, 2617–2627.
- Altringham, J. D. and Ellerby, D. J. (1999). Fish swimming: patterns in muscle function. *J. Exp. Biol.* **202**, 3397–3403.
- Altringham, J. D. and Johnston, I. A. (1990). Modelling muscle power output in a swimming fish. *J. Exp. Biol.* **148**, 395–402.
- Altringham, J. D., Wardle, C. S. and Smith, C. I. (1993). Myotomal muscle function at different locations in the body of a swimming fish. *J. Exp. Biol.* **182**, 191–206.
- Avise, J. C., Nelson, W. S., Arnold, J., Koehn, R. K., Williams, G. C. and Thorsteinsson, V. (1990). The evolutionary genetic status of Icelandic eels. *Evolution* **44**, 1254–1262.
- Bastrop, R., Strehlow, B., Jürss, K. and Sturmbauer, C. (2000). A new molecular phylogenetic hypothesis for the evolution of freshwater eels. *Mol. Phylogenet. Evol.* **14**, 250–258.
- Bone, Q. (1966). On the function of the two types of myotomal muscle fibre in elasmobranch fish. *J. Mar. Biol. Ass. U.K.* **46**, 321–349.
- Coughlin, D. J. and Rome, L. C. (1999). Muscle activity in steady swimming scup, *Stenotomus chrysops*, varies with fiber type and body position. *Biophys. J.* **196**, 145–152.
- Curtin, N. A. and Woledge, R. C. (1996). Power at the expense of efficiency in the contraction of white muscle from dogfish *Scyliorhinus canicula*. *J. Exp. Biol.* **199**, 593–601.
- D'Août, K. and Aerts, P. (1999). A kinematic comparison of forward and backward swimming in the eel *Anguilla anguilla*. *J. Exp. Biol.* **202**, 1511–1521.
- Davies, M. L. F., Johnston, I. A. and Vandewal, J. (1995). Muscle-fibres in rostral and caudal myotomes of the Atlantic cod (*Gadus morhua*, L.) have different mechanical properties. *Physiol. Zool.* **68**, 673–697.
- Eggington, S. (1987). Metamorphosis of the American Eel, *Anguilla rostrata* LeSeur. III. Contractile characteristics of skeletal muscle. *J. Exp. Zool.* **243**, 39–50.
- Ellerby, D. J., Altringham, J. D., Williams, T. and Block, B. A. (2000). Slow muscle function of Pacific bonito (*Sarda chiliensis*) during steady swimming. *J. Exp. Biol.* **203**, 2001–2013.
- Ellerby, D. J., Spierts, I. L. Y. and Altringham, J. D. (2001). Slow muscle power output of yellow- and silver-phase European eels (*Anguilla anguilla*, L.): changes in muscle performance prior to migration. *J. Exp. Biol.* **204**, 1369–1379.
- Gillis, G. B. (1998a). Environmental effects on undulatory locomotion in the American eel *Anguilla rostrata*: kinematics in water and on land. *J. Exp. Biol.* **201**, 949–961.
- Gillis, G. B. (1998b). Neuromuscular control of anguilliform locomotion: patterns of red and white muscle activity during swimming in the American eel *Anguilla rostrata*. *J. Exp. Biol.* **201**, 3245–3256.
- Gillis, G. B. (2000). Patterns of white muscle activity during terrestrial locomotion in the American eel (*Anguilla rostrata*). *J. Exp. Biol.* **203**, 471–480.
- Gray, J. (1946). The mechanism of locomotion in snakes. *J. Exp. Biol.* **23**, 101–120.
- Gray, J. (1968). *Animal Locomotion*. New York: W. W. Norton Co. Inc.
- Grillner, S. and Kashin, S. (1976). On the generation and performance of

- swimming in fish. In *Neural Control of Locomotion* (ed. R. M. Herman, S. Grillner, P. S. G. Stein and D. G. Stuart), pp. 181–201. New York: Plenum.
- Hammond, L., Altringham, J. D. and Wardle, C. S.** (1998). Myotomal slow muscle function of rainbow trout *Oncorhynchus mykiss* during steady swimming. *J. Exp. Biol.* **201**, 1659–1671.
- Jayne, B. C. and Lauder, G. V.** (1995). Are muscle fibers within fish myotomes activated synchronously? Patterns of recruitment within deep myomeric musculature during swimming in largemouth bass. *J. Exp. Biol.* **198**, 805–815.
- Johnson, T. P., Syme, D. A., Jayne, B. C., Lauder, G. V. and Bennett, A. F.** (1994). Modeling red muscle power output during steady and unsteady swimming in largemouth bass. *Am. J. Physiol.* **267**, 418–488.
- Johnston, I. A., Davison, W. and Goldspink, G.** (1977). Energy metabolism of carp swimming muscles. *J. Comp. Physiol.* **114**, 203–216.
- Johnston, I. A., Franklin, C. E. and Johnson, T. P.** (1993). Recruitment patterns and contractile properties of fast fibres isolated from rostral and caudal myotomes of the short horned sculpin. *J. Exp. Biol.* **185**, 251–265.
- Josephson, R. K.** (1985). Mechanical power output from striated muscle during cyclic contractions. *J. Exp. Biol.* **114**, 493–512.
- Knower, T., Shadwick, R. E., Katz, S. L., Graham, J. B. and Wardle, C. S.** (1999). Red muscle activation patterns in yellowfin (*Thunnus albacares*) and skipjack (*Katsuwonus pelamis*) tunas during steady swimming. *J. Exp. Biol.* **202**, 2127–2138.
- Lindsey, C. C.** (1978). Form, function and the locomotory habits in fish. In *Fish Physiology*, vol. VII (ed. W. S. Hoar and D. J. Randall), pp. 1–100. New York: Academic Press.
- Long, J. H.** (1998). Muscles, elastic energy and the dynamics of body stiffness in swimming eels. *Am. Zool.* **38**, 771–792.
- Mosauer, W.** (1932). On the locomotion of snakes. *Science* **76**, 583–585.
- Pankhurst, N. W.** (1982). Changes in body musculature with sexual maturation in the European eel *Anguilla anguilla* (L.). *J. Fish Biol.* **21**, 417–428.
- Rayner, M. D. and Keenan, M. J.** (1967). Role of red and white muscles in the swimming of the skipjack tuna. *Nature* **214**, 392–393.
- Rome, L. C., Choi, I., Lutz, G. and Sosnicki, A.** (1992). The influence of temperature on muscle function in the fast swimming scup. I. Shortening velocity and muscle recruitment during swimming. *J. Exp. Biol.* **163**, 259–279.
- Rome, L. C., Swank, D. and Corda, D.** (1993). How fish power swimming. *Science* **261**, 340–343.
- van Leeuwen, J. L., Lankheet, M. J. M., Akster, H. A. and Osse, J. W. M.** (1990). Function of red axial muscles in carp (*Cyprinus carpio* L.): recruitment and normalised power output during swimming in different modes. *J. Zool., Lond.* **220**, 123–145.
- Wardle, C. S. and Videler, J. J.** (1993). The timing of the electromyogram in the lateral myotomes of mackerel and saithe at different swimming speeds. *J. Fish Biol.* **42**, 347–359.
- Wardle, C. S., Videler, J. J. and Altringham, J. D.** (1995). Tuning in to fish swimming waves: body form, swimming mode and muscle function. *J. Exp. Biol.* **198**, 1629–1636.
- Wardle, C. S., Videler, J. J., Arimoto, T., Franco, J. M. and He, P.** (1989). The muscle twitch and the maximum swimming speed of giant bluefin tuna, *Thunnus thynnus* L. *J. Fish Biol.* **35**, 129–137.
- Webb, P. W.** (1978). Hydrodynamics: Nonscombroid fish. In *Fish Physiology*, vol. VII (ed. W. S. Hoar and D. J. Randall), pp. 190–239. New York: Academic Press.
- Williams, G. C. and Koehn, R. K.** (1984). Population genetics of North Atlantic catadromous eels (*Anguilla*). In *Evolutionary Genetics of Fishes* (ed. B. J. Turner), pp. 529–560. New York: Plenum.
- Williams, T. L., Grillner, S., Smoljaninov, V. V., Wallen, P., Kashin, S. and Rossignol, S.** (1989). Locomotion in lamprey and trout: the relative timing of activation and movement. *J. Exp. Biol.* **143**, 559–566.